11-4-2014

Aerodynamic Optimization of Box Wing – A Case Study

Adeel Khalid
Embry-Riddle Aeronautical University - Worldwide, khalida1@erau.edu
Parth Kumar
Cambridge High School, pkumar75@gatech.edu

In recent decades, the market for aircraft and aircraft transport has increased tremendously, and this has resulted in an increase in emissions, fuel consumption, and the cost. In order to reverse this increasing trend, various companies have researched methods of reducing drag in order to maximize the lift to drag ratio. Examples of aircraft that have recently been developed or are in development with new technologies the Boeing 787-8 Dreamliner and the Airbus A350 XWB. While many of these aircraft incorporate new technologies, the overall cantilever configuration has remained largely the same and it is nearing a point of minimal returns for great development costs (Cuerno-Rejado, 2009). In order to significantly improve the potential of aircraft, a different configuration may be beneficial; however, the problem arises involving integration with today's aviation world. The flying wing and blended wing body are two popular designs that have been researched, with low drag and high lift, but these will require significant changes to existing airports and manufacturing lines in order to be feasible, not to mention unfavorable stability and control characteristics. In contrast to the blended wing configurations, non-planar wing designs offer significant commonality with the cantilever configurations in use today, while still providing a significant drag reduction (note: For all formulas and computations, see appendix for nomenclature).

Non-planar aircraft configurations, including the ring wing and the box wing, among others, aim principally to minimize induced drag by fundamentally being an extension of the winglet. The ring-wing design is largely infeasible, due to its lack of suitable positions for landing gear, among other reasons. However, the other two designs have been researched more extensively, with several companies and individuals conducting research upon them[2]. The box wing is similar to a biplane, but the upper and lower wings are connected at the tip and may be staggered to create wind sweep. As far back as 1924, Ludwig Prandtl had researched the box wing configuration, due to it being the "best wing system", or theoretically having the least induced drag (Prandtl, 1924) (Shiktanz, Master's Thesis, Dept. of Automotive and Aeronautical Engineering, Hamburg University of Applied Sciences). Along with aerodynamic benefits, this wing system employs other benefits, such as reduced weight, and increased control surfaces leading to good control and stability characteristics. Until recently, the box wing was an unlikely configuration for large commercial aircraft due to the large amount of parasitic drag that would result from structural supports. Recent advances in composite materials have made these designs a more probable solution to improving aircraft performance, for now supports are not needed.

An example box wing configuration is developed in this project through iterative optimization. The role of the box wing is medium range commercial flight, and cruise flight performance is maximized through increasing the lift to drag ratio.

The Box Wing Concept

Drag Characteristics

One of the primary improvements the box wing provides is a significant reduction in induced drag. Induced drag occurs due to the vortices generated at the tip of the wing, and can account for almost 40% of cruise drag produced and an even larger percentage of the drag produced at takeoff (Kroo I. , 2005). In addition to improving overall efficiency, reducing the drag produced at takeoff allows design changes not previously possible, allowing for greater savings in cruise. Some sources indicate a 20-30% decrease in induced drag (Cuerno-Rejado, 2009) (Kroo I. , 2005).

Several factors are involved to give the box wing such low induced drag. The span efficiency factor *e* is inversely proportional to the induced drag coefficient, and equals one for an elliptical lift distribution (i.e. an elliptical wing). For biplanes, it can be shown that the span efficiency factor can be greater than one, giving these aircraft significantly less induced drag. Box wing aircraft joined at the tip benefit the most from this, whereas inboard joined wings can greatly reduce the factor *e* to where the induced drag is not significantly less than that of a conventional aircraft. In addition, both wings should produce the same amount of lift for the optimum lift distribution, although this may not always be possible.

The trim drag of an aircraft is essentially the induced drag of the control surfaces. For tip-joined configurations, the increase in induced drag is quite small, and for an inboard-joint configuration it is approximately equivalent to that of a conventional aircraft, and is not a major component of drag.

The interference of the airflow caused by the fuselage decreases the efficiency of the box wing, as with any aircraft. In box wings, the rear wing suffers much less from this interference, due to it being behind the fuselage, allowing it to perform more optimally. This allows the effect of the fuselage on efficiency to essentially be cut in half when compared to conventional aircraft. Despite this, the box wing has another factor to increase interference: with any design with multiple wings, it is necessary to consider interference between the

airflows of the front and back wings. Wind tunnel experimentation suggests that the drag is not significantly increased by interference, likely due to the lack of a wing overlap in plan view of the models tested in those experiments, suggesting that a large increase in winglet height may not provide significant benefits for interference drag (Wolkovitch, 1986).

The early biplanes, while granting reduced induced drag, suffered from large amounts of parasitic drag due to supports and bracing. Today, with the advent of composites and stronger materials, box wings can be built without the need for supporting structures, greatly reducing parasitic drag when compared to biplanes of the time. Compared to most modern cantilever aircraft, the box wing will have greater wetted area, and thus a larger amount of parasitic drag. In addition, box wings generally have smaller chord lengths than corresponding conventional aircraft, due to the wing area being split over two wings. The primary result of this is a decrease in the Reynolds number, which results in higher viscosity and increased skin friction drag.

To minimize interference drag, it has already been discussed to not overlap the wings in plan view (Wolkovitch, 1986). In addition, to lower parasite drag, the front wing root should join to the fuselage at a location with a favorable pressure gradient in order to reduce flow separation at that point. In addition to this, the use of laminar flow airfoils may be desirable, due to the lower Reynolds numbers of box wings.

During transonic and supersonic flight, the compression of shock waves in front of the aircraft will form a major component of the total drag, known as wave drag. At the high speeds that commercial airliners travel at, it becomes essential to account for this. In most conventional aircraft, this is countered partially, but not entirely, by sweeping back the wings. Another way that can lead to a reduction in wave drag is the use of very thin airfoils, made possible by the structural strength of the box wing. In addition to this, box wing aircraft match the area rule more closely than conventional aircraft, allowing for a more ideal area distribution at high speeds.

Lift Characteristics

One of the advantages that a box wing aircraft has is a relatively high trimmed $C_{L,MAX}$. In box wing aircraft the front wing will stall first, with the rear wing still far from stalling. This is advantageous in the sense that it allows the aircraft to have good stability properties, giving it a higher trimmed $C_{L,MAX}$, but also is disadvantageous because some of the potential of the rear wing is wasted.

To satisfy this problem, the rear wing should be designed such that the front wing will stall only when the rear wing is generating most of its lift, such that little of the potential of the rear wing is wasted and the stability advantage remains.

To maximize the rear wings $C_{,LMAX}$, several changes to the aircraft geometry can be utilized. Decreasing the sweep of the rear wing, increasing the ratio of the rear wing chord to the front wing chord, and moving the Aerodynamic Center (A.C) and Center of Gravity (C.G) aft all help do this. In addition to modifying airframe geometry, it is essential that the airfoils be selected properly.

According to Wolkovitch (Wolkovitch, 1986), the design of airfoils for box wing airfoil must take into account the flow induced by the wings on each other. In regards to airfoil design specifically for box wing aircraft, little else has been done about the topic; however, biplane airfoils may be useful in optimizing this aircraft[6]. Biplanes are also affected by many of the same interferences forces, and also have induced airflows.

The addition of a canard with high sweep can help to augment the lift, as well as improve the controllability of the aircraft. According to wind tunnel experimentation, a box wing with a canard had a lift coefficient nearly 20% greater than that of a conventional aircraft with the same lifting area, and about 15% greater than that of a traditional box wing with equivalent lifting area (Wolkovitch, 1986).

General Design of the Test Model

The box wing aircraft in this experiment is designed to act as a medium to large capacity, long-range aircraft. The maximum takeoff weight (MTOW) of the design is 250,000 kg (551,156 lbs.) and the maximum range with payload is 13,500 km (8388 mi). Current comparable cantilever aircraft are listed in Table 1.

Table 1

Comparison of Aircraft with Similar Missions

	A330-200[1]	A340-300[4]	A350-800[5]	Boing 787[6]	Il-96-300[7]
MTOW	242,000 kg	275,000 kg	248,000 kg	227,930 kg	250,000 kg
Max Range	13,400 km	13,700 km	15,300 km	14,200-15,200 km	13,500 km
Length	58.82 m	63.39 m	60.54 m	57 m	55.345 m
Wingspan	60.30 m	60.30 m	64.75 m	60 m	60.105 m
Height	17.39 m	16.91 m	17.05 m	17 m	17.55 m
Fuselage Width	5.64	5.64 m	5.96 m	5.74 m	6.08 m

The baseline cantilever aircraft is the Airbus A330-200, due to the similarities between A330-200 and the suggested mission profile for this box wing. The length, wingspan, wing area, and height of the box wing aircraft are all matched to that of the Airbus A330-200.

The two wings should be joined near the end of the wing, with the tip-joined configuration employing several aerodynamic advantages over the inboard joined; however, the tip-joined has greater weight. The optimal configuration results between 50%-100% of the wing semi-span (Wolkovitch, 1986) (Gallman, 1993). For this experiment, aerodynamics is the primary consideration and the tip-joined wings are used in this box wing aircraft. In addition, moving the aerodynamic center back allows for improvements in stability and control, as well as with optimizing the lift production of the wing (Cornille, 1999) (Shiktanz,

---

[1] From http://www.airbus.com/aircraftfamilies/passengeraircraft/a330family/a330-200/specifications/

[4] From http://www.airbus.com/aircraftfamilies/passengeraircraft/a340family/a340-300/specifications/

[5] From http://www.airbus.com/aircraftfamilies/passengeraircraft/a350xwbfamily/a350-800/specifications/

[6] From http://www.boeing.com/boeing/commercial/787family/787-8prod.page

[7] From http://www.ilyushin.org/en/aircrafts/passenger/1174/

Master's Thesis, Dept. of Automotive and Aeronautical Engineering, Hamburg University of Applied Sciences), and is accomplished through employing a rear wing with less sweep. To keep the aircraft's benefits with regards to the area rule, utilizing a relatively smaller back wing offsets the different wing sweep (Shiktanz, Master's Thesis, Dept. of Automotive and Aeronautical Engineering, Hamburg University of Applied Sciences) (Wolkovitch, 1986). Lastly, maximization of the longitudinal distance between the two wings is optimal; however, the winglet size and sweep provides a limiting factor (Shiktanz, Master's Thesis, Dept. of Automotive and Aeronautical Engineering, Hamburg University of Applied Sciences). For the purposes of this experiment, the winglet sweep is set at 30 degrees. To place the front wing in an area of "favorable pressure gradient" (Wolkovitch, 1986), the root of this wing is moved near the front, which will increase longitudinal distance as well.

The span is set similar to the conventional airliners, and the winglet height is set as 20% of the span for the purposes of the preliminary airfoil selection. For the 2nd and 3rd stage of optimization, the aspect ratio and the winglet height are varied to find the optimal values for these specific parameters.

CFD Validation

The purpose of the validation is to calibrate the software to be accurate against published data. The CFD program used in this experiment is Dassault Systèmes SolidWorks Flow Simulation. Validation is conducted by comparing C_L and C_D values of the airfoil NACA 0009 with published data from Abbot (Abbot, 1959). The Reynolds number for validation of the airfoil is 6 million, and is compared to published data of the same Reynolds number.

The CFD analysis in this experiment utilizes an external analysis with internal space excluded, default gravity, air as the fluid, P=101,325 Pa, T=298.2 K, v=9.289752398 m/s. The computational domain is set at approximately 140 meters by 80 meters, with a depth of 0.1 meters. The analysis is set to 2D for the purposes of the airfoil. The reason for this is to exclude the induced flow effects. Most airfoil polars exclude 3-D wings effects as well, including those in Abbott (1959). The chord length of the airfoil is 9.754 meters.

Using the formula for Reynolds number, it can be seen that:

$$Re = \frac{\rho vc}{\mu} = \frac{vc}{\nu} = \frac{9.289752398\frac{m}{s} * 9.754m}{1.511 * 10^{-5}\frac{m^2}{s}} = 6 * 10^6$$

The lift coefficient is calculated as follows:

$$C_L = \frac{2L}{\rho v^2 S} = \frac{2L}{1.225\frac{kg}{m^3} * 9.289752398^2\frac{m^2}{s^2} * (.1\,m * 9.754\,m)}$$

Note that $S = .1 * 9.754$, as 0.1 is the depth of the computational domain. Lift is calculated through setting the CFD software to compute it, with drag and the drag coefficient were done similarly. The CFD analysis is conducted at 5 different angles of attack: -12, -8, 0, 8, and 12. All parameters were left the same between cases. The computation took approximately 2 hours on Quad Core Intel Xeon W3530 at 2.8 Ghz. The resolution of the mesh was set manually at 800 by 300 cells, with a small surface refinement level of 2. All other parameters were set to default.

Validation Results

The lift coefficient data follows the proper trend, showing a clear linear relation, and in terms of absolute numerical value is the CFD analysis is also fairly accurate. Note that the CFD solver does not perform extremely well at negative angles of attack, likely as a result of flow separation, shown in Fig. 1. This does not affect this experimentation significantly, for in general airliners do not cruise at negative angle of attacks, and when the aircraft do, the wings are still at a positive incidence angle. The drag coefficient follows the correct trend as well, with a roughly parabolic graph with vertex at α equals 0 degrees. Clearly, the CFD greatly overestimates the drag. (Fig. 2)

At 0 degrees, the CFD analysis performs most accurately, with the experimental data being about 1.3 times that of the theoretical. At other angles of attack, the ratio is much greater, likely being a result of the complexity of drag calculations and flow separation. Clearly, the CFD analysis is capable of showing the correct trends, and giving the basis for providing a comparison between different cases within this same experiment.
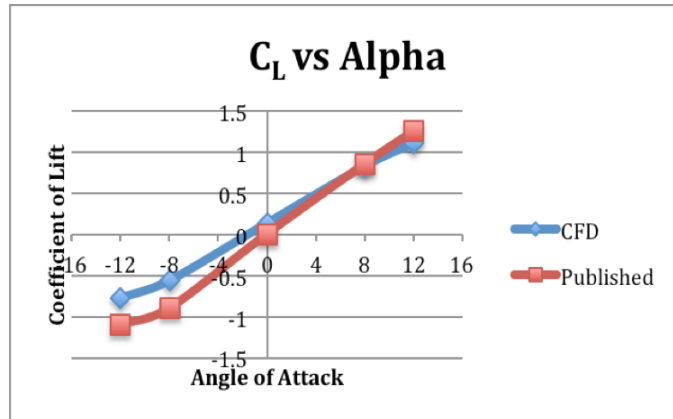
Figure 1. C_L vs. α results. The graph shows that the CFD analysis software correctly computed the amount of lift generated.
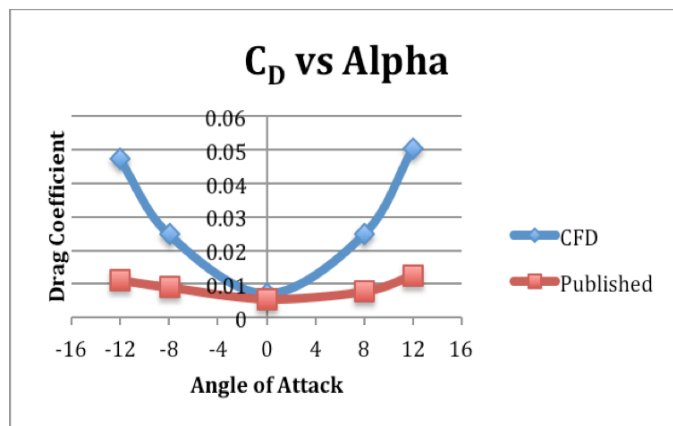

Figure 2. C_D vs. α results. The graph shows that the CFD analysis software correctly computed the trend for the amount of drag, but not the absolute amount generated.

In conclusion, the CFD analysis is capable of calculating lift's absolute value, and is capable of giving an accurate trend in drag. As a result, the C_L/C_D curve has the correct trend as well. Because this experiment involves the maximization of C_L/C_D, the accuracy of its trend is most important, and as such the data obtained from the solver in later stages will have sufficient to perform a relative analysis.

Preliminary Airfoil Optimization

Little research has been done on airfoil optimizations for the box wing aircraft. A preliminary analysis of select airfoils is performed in the first stage of optimization, using airfoils from different aircraft of similar speeds and roles.

Airfoil Selection for 1st stage of Optimization

In order to select the appropriate airfoils for the box wing, a variety of considerations had to be made. As this is an optimization of cruising speed performance, the box wing will travel at speeds near Mach 0.85. As a result, the airfoils must be supercritical airfoils, which have reduced wave drag. In addition to this, different airfoils have been optimized at various Reynolds numbers. The Reynolds number for box wing aircraft is significantly lower than that of airliners of similar size, due to the wing area being split between the forward and aft wings. Lastly, high lift airfoils are desirable. In some conventional airliners, the tip airfoil is made to produce less lift than the root airfoil in order to create a more elliptical distribution of lift to lower induced drag. This is not a consideration for the box wing, which anyways has a low amount of induced drag. For the cantilever A330-200, the airfoil data is likely proprietary and not released. As a result, the BAC J airfoil used on the Boeing 747 is used for the cantilever model, both being larger commercial airliners.

Two models are tested to act as controls to compare box wing performance between various airfoil types. The first is the box wing with simply a BAC J airfoil on both the root and tip, for comparison against the cantilever with the same airfoil. The second is the box wing with the Clark Y airfoil on both the root and tip. The Clark Y is not a supercritical airfoil; however, it is an airfoil commonly used in biplanes.

There are three more models with the same root and tip airfoils. The first is the KC-135 Winglet Airfoil. This supercritical airfoil is quite thin, with a thickness to chord ratio of 8%, which results in low drag. In addition, the airfoil may perform well at this range of Reynolds numbers, as the winglet of the KC-135 has a chord length similar to that of the box wing designed for this study. Lastly, this airfoil is designed to perform well in an area of interference, between the winglet and wing, which may give it favorable characteristics in a box wing aircraft, which has interference between the forward and aft wings. The next airfoil in this category is the DSMA-523 airfoil. This airfoil is solely picked for being a supercritical airfoil used on similarly sized aircraft. The last airfoil in this category is the SC(2)-0412 airfoil. It is a thicker airfoil, with a thickness to chord

ratio of 12%, and is included as no other airfoil in this experiment has as thick of a leading edge.
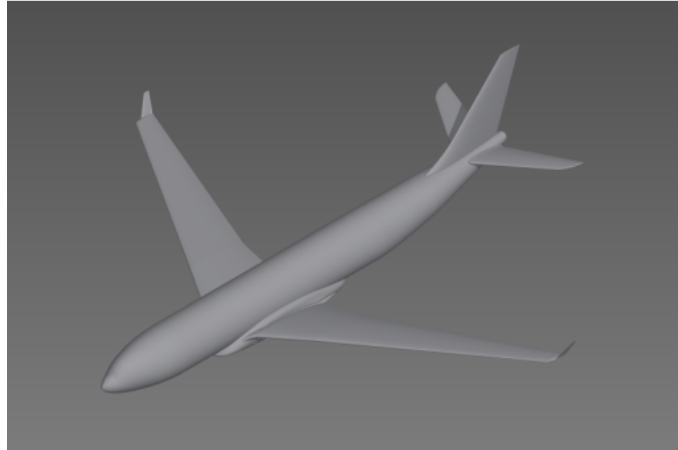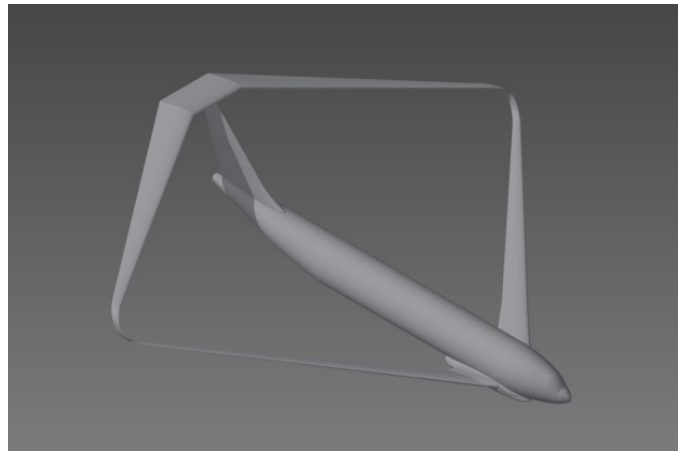

Figure 3. Cantilever CAD Model.

Figure 4. BAC J Baseline CAD Model.

The final category of models have variable root to tip airfoils. The advantage of this is that each position from the root to the tip is optimized for its respective Reynolds number, assuming that both the root and the tip airfoils are as well. There are 3 cases in this category.

The first model utilizes the midspan airfoil of the 737 on the root of the box wing, and the 737 tip airfoil on the box wing tip. The respective Reynolds

numbers were compared, and were found to match well for the box wing. The second utilizes a KC-135 .32 airfoil on the root, and a KC-135 winglet airfoil on the tip, for the same reason as above.

The final airfoil is designed in the software XFLR5. Considerations from are used to design both the root and the tip foils (Abbot, 1959). The tip airfoil is a heavily modified KC-135 winglet airfoil. The root airfoil is designed separately. The coordinates for the KC-135 Winglet are exported into the XFLR5 software, and the camber of the airfoil is increased to create a tip airfoil. The root airfoil is developed as a thicker version of the tip. This software is utilized due to its ability to generate coordinates to import into Autodesk Inventor.

Note that it is difficult to consider the lift and drag coefficient values of the airfoils, as data does not exist or is not available for many airfoils at the Reynolds numbers commercial airliners cruise at. While the lift coefficient does not vary greatly with Reynolds number, it would not necessarily be accurate to take data at ~1 million Re and assume it true for greater than 40 million.

Airfoil Optimization Methodology

This optimization is conducted on a box wing at conditions simulating an Airbus A330-200 in cruise at 11,000 meters, 4 hours into flight. An example of such a flight would be between New York and Berlin. The fuel consumption of an Airbus A330-200 is approximately 5,300 kg/h[8], and when initially loaded near max takeoff weight is about 232,000 kg. Thus the cruise weight for an aircraft at these conditions is near 210,000 kg.

A total of 9 different models are designed in the CAD software Autodesk Inventor. Utilizing available dimensions and 3 views, an Airbus A330-200 model is created, with the (Cornille, 1999) BAC J airfoil as both the root and the tip airfoil. 6 degrees incidence angle on the root and 4 degrees on the tip is utilized in the model. Note that the model is designed with a wing span of 60 meters as a result of utilizing CFD analysis.

After the creation of the cantilever model using the BAC J airfoil, the box wing base model is designed. The parameters match those in the review of literature, and all the incidence angles, fuselage models, vertical stabilizers, etc. remain constant between the models. The box wing base model also utilizes the BAC J airfoil on both the root and tip for the front and aft wings. All of the other 7 CAD box wing models are variations of this model. Four models consisted of

the following four airfoils being used at both the root and the tip of the front and aft wing: the KC-135 Winglet, the SC(2)-0412, the DSMA-523A, and the Clark Y. Three models had varied airfoils at the root and the tip: the KC-135 BL124.32 airfoil at the root of both wings, and the KC-135 Winglet airfoil at the tip of both wings; 737 midspan airfoil at the root of both wings, and the 737-tip airfoil at the tip of both wings; and the designed airfoils model. A single airfoil set is created using XFLR5, as outlined above.

After designing all the models in Autodesk Inventor, the models are exported to Dassault Systèmes SolidWorks for CFD analysis. Cruise conditions at 11,000 meters are P=22,633 Pa and T=216.65 K, with v=250 m/s. In order to allow for more rapid computation, CFD analysis is performed on only one half of the model, and a symmetry boundary condition is used on the symmetry plane.

At cruise conditions, the lift generated by an aircraft is only sufficient to cancel the weight, as any extra lift will result in the aircraft continuously climbing. Aircraft with high lift to drag ratios can fly at low angle of attacks to decrease drag and have sufficient lift. In order to find the angle of attack that would result in the same lift as the weight of a model, a C_L vs. α relation is created by conducting CFD analysis at 0 degrees angle of attack and then 3 degrees angle of attack. Utilizing the following formula, the C_L values can be computed for the 0 degrees and 3 degrees angle of attack cases.

$$C_L = \frac{2L}{\rho v^2 S}$$

S is computed through area calculation features of the CAD software; however, it can also be assumed to be 1, and will not affect the computation of the desired angle of attack in the end. From this equation, the C_L values are calculated from the two previous data points and a C_L vs. α relation of the form C_L=$m\alpha$+b is formed.

In order to analyze design point and off design point cruise performance, the required C_L values for 225 m/s, 237.5 m/s, 250 m/s, 262 m/s, and 275 m/s. cruising speeds are found, which lead to the corresponding α values from the relation found previously. Original considerations assumed a weight of 210,000 kg, so thus the lift force must be 2,059,396 N. In addition, it is assumed that C_L vs. α remains roughly linear regardless of Reynolds number, and as such the following formula is created:

$$C_L = \frac{2L}{\rho v^2 S} = \frac{2{,}059{,}396.5}{.3692 * v^2 S}$$

From the above expression, all angles of attack are calculated for different cruising speeds. This is repeated for every model separately, yielding a total of 7 cases per model (or 63 total cases). Note that the analysis is conducted on half the model in order to speed up computation, and thus the lift force in the equation is half of the total needed.

Airfoil Optimization Results

Table 2
Lift results for Airfoil Optimization

Lift (N)	0° Cruise	3° Cruise	225 m/s	237.5 m/s	250 m/s	262.5 m/s
737	805820	1055183	997790	937005	1036807	1038967
BAC J	751013	1098369	927900	894907	1011382	985079
Clark Y	873271	1192221	1003998	984938	1006807	1036888
Designed	837026	1206881	1028669	1028669	1041287	1054522
DSMA	566326	838936	871069	916861	1008444	981502
KC-135 .32	786754	1019628	1018872	1010013	1031004	1080049
KC-135 Winglet	961772	1208696	1104278	1007362	1070683	1020063
SC(2)-0412	668163	964589	945765	942433	934317	1057808
Cantilever	830545	1150151	1064575	998929	1053817	1035675

Table 3
Drag results for Airfoil Optimization

Drag (N)	0° Cruise	3° Cruise	225 m/s	237.5 m/s	250 m/s	262.5 m/s	275 m/s
737	230641	299148	275824	278893	289168	283843	300244
BAC J	158648	231513	219059	209244	213272	220597	228096
Clark Y	214574	288354	241693	239244	279845	278147	278870
Designed	216865	272246	223715	223715	233345	252946	270024
DSMA	177322	225153	278916	257792	279456	279714	289434
KC-135 .32	206533	266872	275210	247427	273576	272282	281720
KC-135 Winglet	163942	244824	210304	194099	184513	187160	189559
SC(2)-0412	188518	252024	257196	255167	296332	278855	292081
Cantilever	165240	233215	205463	187980	201285	215421	240664
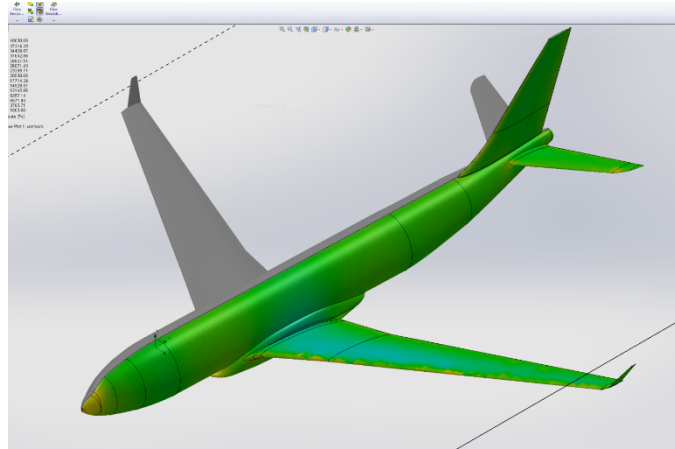
Figure 5. Cantilever Pressure Plot. *1000-40,000 Pa*
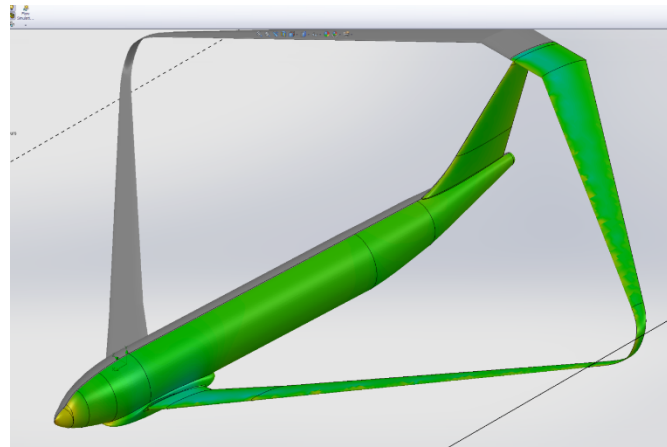
Figure 6. BAC J Baseline Pressure Plot. *1000-40,000 Pa*
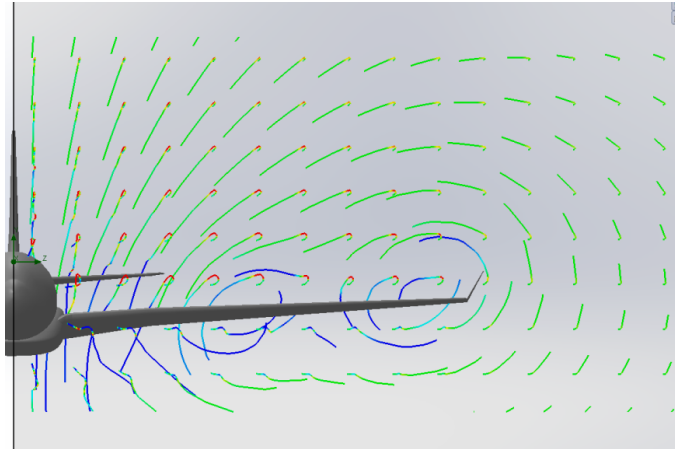
Figure 7. Cantilever Flow Trajectory. *240-260 m/s*
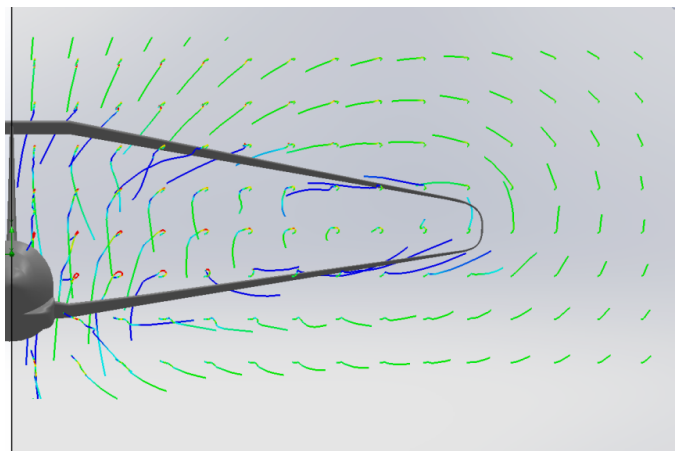
Figure 8. BAC J Baseline Flow Trajectory. *240-260 m/s*
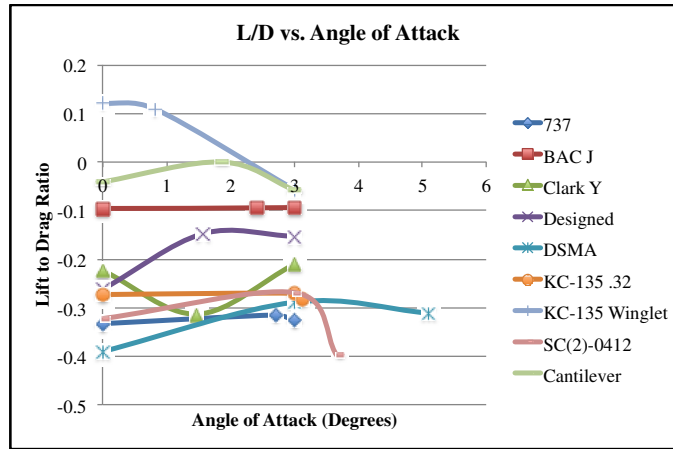
Figure 9. Lift to Drag vs. *α. Airfoil*
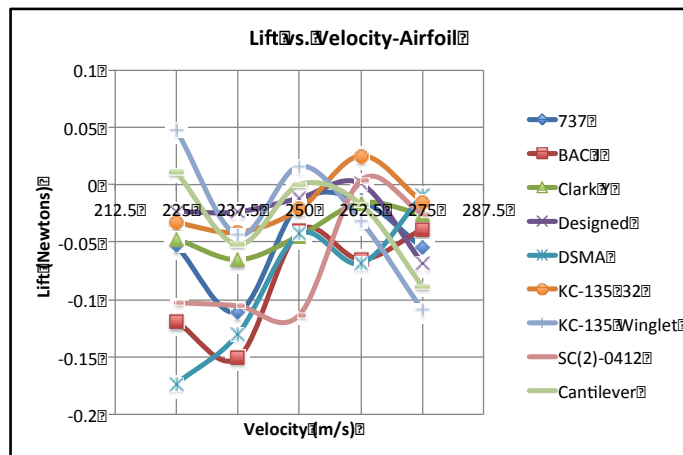
Figure 10. Lift vs. Velocity. *Airfoil.*

Airfoil Optimization Data Analysis

A total of 9 different models, 8 box wings and 1 cantilever wing model, are tested in a CFD analysis. 7 different cases are done: 0 degrees angle of attack, 250 m/s airspeed; 3 degrees angle of attack, 250 m/s; and 5 different cases with a calculated angle of attack at the speeds of 225 m/s, 237.5 m/s, 250 m/s, 262.5 m/s, and 275 m/s. All the cases are done at atmospheric conditions at 11,000 meters, with pressure at 22,633 Pa, and temperature at 216.65 K. The lift and drag values are given in Newtons. All the models perform fairly well, with every model maintaining a lift to drag ratio above 3 in all cases, as a result of the examination

made when selecting airfoils. From the CFD validation, it is clear that SolidWorks CFD does not allow for absolute comparisons, only relative comparisons, so thus all of the following graphs are normalized with respect to the cantilever configuration at cruise conditions, with 0 being the lift, drag, and lift to drag ratio values at that point. For example, a lift of .1 means a lift 10% higher than the cantilever at 250 m/s cruise angle of attack.

Clearly, the model with the greatest performance is the box wing with the KC-135 Winglet airfoil. In 6 out of 7 cases, it has the highest lift to drag ratio out of all the models, only being exceeded by the cantilever wing model at the airspeed of 237.5 m/s. The model that comes closest to the KC-135 Winglet is the cantilever model. Examining the model's lift to drag ratio shows that there is only one case where a model other than the box wing KC-135 Winglet has a greater lift to drag ratio-at the highest speed tested, 275 m/s, the box wing BAC J has a higher lift to drag ratio.

The box wing BAC J airfoil and the box wing designed airfoil both follow the other two models, in most cases having the third and the fourth highest lift to drag ratios respectively. The box wing designed performs well at low speeds less than 250 m/s, having a lift to drag ratio above the BAC J, but at higher speeds has lower performance. At higher angles of attack it seems to improve in comparison to the BAC J airfoil, but not significantly (See Fig. 11).
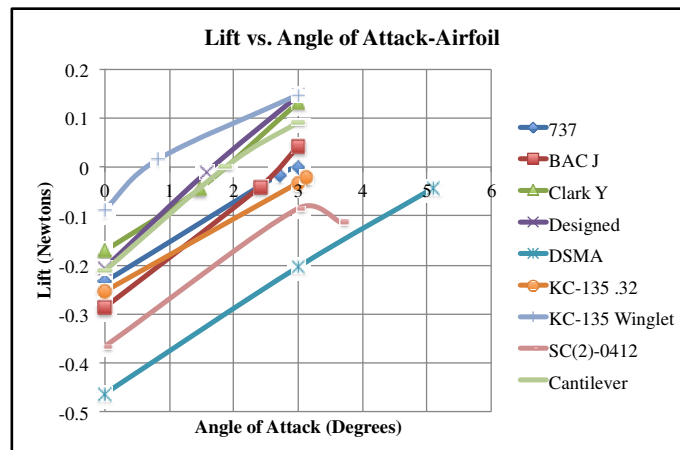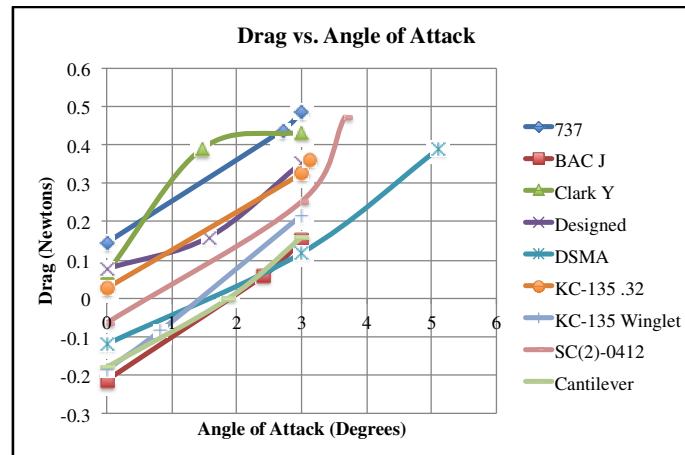

Figure 11. Lift vs. *α. Airfoil*

Figure 12. Drag vs. *α. Airfoil*

The other models start having much more variable data. Primarily the box wing KC-135 .32 performs better than the others, more so by being quite constant in its lift to drag ratio across various conditions. The Clark Y follows, and after this the last three models are very close.

In terms of the cruise condition for which the box wing is being optimized, at 250 m/s, the KC-135 Winglet airfoil outperforms the rest, with a lift to drag ratio about 10% higher than that of the cantilever aircraft. After that, the next highest is the baseline airfoil design.

Examining Figure 12, there is not a significant amount of change in lift, as expected, with the primary exceptions at 225 m/s and 237.5 m/s, where likely the angle of attack was too high and resulted in flow separation. The lift vs. angle of attack is different, with a lot of change. Nearly all the models had an approximately linear lift vs. α curve, in accordance to the calculations made. In general, the order of highest lift to lowest lift airfoil did not change across the x-axis significantly; however, one noticeable difference between this graph, the drag vs. α, and the lift to drag ratio vs. α is that the cantilever is towards the middle for the amount of drag produced, rather than the top, being beaten by the box wing KC-135 Winglet, the box wing designed, and the box wing Clark Y.

First, the Clark Y and BAC J are analyzed. The box wing Clark Y was the only airfoil tested that was not optimized for flight at such high Reynolds numbers. Comparing the lift values in Fig. 13, the Clark Y airfoil clearly produces a large amount of lift, greater than most models, as a result of the large amount of camber on the airfoil. To compensate for this, the drag is high as well. This is a direct result of the fact that it is not supercritical, and thus the wave drag is very high. This is also visible in the drag vs. velocity graph.

One of the most important benefits of the box wing is the low induced drag. Comparing the drag produced in Fig. 14 for the cantilever wing and the other box wings, it is visible that the cantilever had lower drag than most of the models; however, comparing the box wing BAC J, which shared the same airfoil as the cantilever, it is visible that the cantilever here had a slightly higher drag value. This was more than compensated for by the higher angles of attack the box wing BAC J had to travel at to maintain the 2,059,396.5 Newtons of force, leading to its higher drag in Fig. 15, drag vs. velocity (below). The lesser lift for the box wing as compared to the cantilever was likely a result of the airfoil not being optimized for the lower Reynolds number, being a 747 airfoil. This also ended up likely increasing the drag of the box wing, although the amount by which it did is unknown.

Both the box wing DSMA-523 and the box wing SC(2)-0412 performed poorly. For the box wing SC(2)-0412, this is a direct result of the large amount of drag produced, which in turn was created by the thickness of the airfoil. The symmetry of the airfoil may have helped reduce the lift created by the airfoil. Note that while the airfoil was at an angle of incidence, the lower camber can still cause a reduction in lift. As a result of the low lift produced by the box wing SC(2)-0412, this resulted in high angles of attack being necessary for production of the necessary amount of lift. The box wing DSMA did produce very low drag; however, it also produced very low lift at 0 degrees and 3 degrees angle of attack, the least lift of any model. This resulted in high angles of attack for the model to maintain the proper amount of lift at cruising conditions, for the same reason that the box wing SC(2)-0412 performed poorly. This is why both models perform poorly in the Figure 12.
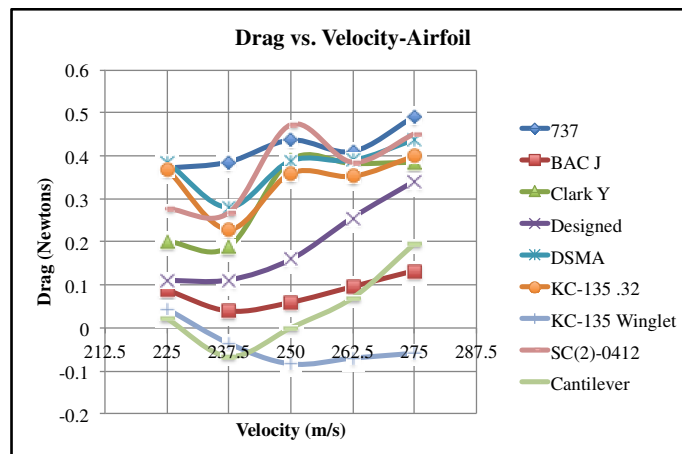

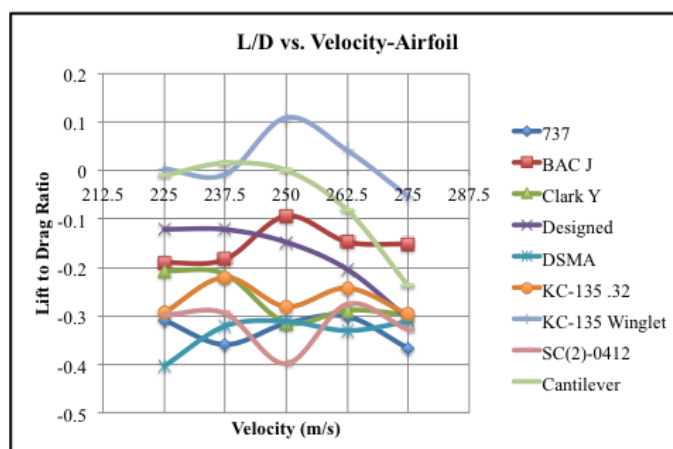
Figure 13. Drag vs. Velocity. *Airfoil*

Figure 14. Lift to Drag vs. Velocity. *Airfoil*

The box wing with a designed airfoil produced a large amount of lift, but in addition it produced great amounts of drag. Likely this was a result of the root airfoil, being thicker than the BAC J airfoil, about the same thickness as the box wing SC(2)-0412 model, which produced a great amount of drag, as discussed above. The root airfoil could have been modified to allow the model to possibly reduce drag. Iterative modifications may result in making an airfoil that can outperform the box wing KC-135 Winglet model.

The box wing with a 737 airfoil performed much worse than expected. Having different root and tip airfoils, each optimized for the proper Reynolds number, led to the hypothesis of it having a high lift to drag ratio. More than likely, the reason for this is not in the Reynolds number, but rather the cruise speed of 250 m/s that this experiment used. The 737 from which the airfoil was taken from cruised at a speed lower than most modern airliners, less than Mach .75. This likely led to it not being affected as much by wave drag, and as such the airfoils were not very effective at countering it. The airfoils show that both the root and tip have much less distinctive supercritical features than the other airfoils. This led to poor lift and drag performance at 0 and 3 degrees, 250 m/s, which led to high angles of attack for the lift vs. velocity curve.

The last model with variable airfoil is the KC-135 .32. This particular model performed almost in the middle, as the "average" of the rest of the models. This can likely be explained due to the root and the tip airfoils used. The tip airfoil was the KC-135 Winglet, and allowed a greater amount of lift production as compared to other models; however, the root airfoil compensated for this.

Comparing data for low Reynolds numbers, it is still visible that the KC-135 .32 airfoil used on the root had a lower lift coefficient than comparable airfoils. While the lift coefficient may not always scale well across Reynolds numbers, here this may be the cause. In addition, the greater lift produced on the tips likely would have created an opposite effect compared to an elliptical lift distribution, reducing the induced drag benefit and increasing overall drag. Possibly putting a high lift root airfoil would be beneficial, when coupled with the KC-135 Winglet on the tip.

Finally, the model that performed the best must be analyzed. The KC-135 Winglet had a significantly larger lift to drag ratio than the other models. This is likely a combination of factors, and likely a combination of the reasons for which it is one of the airfoils even tested. The thinness allowed for low wave drag; however, the fact that it performed well in an area of interference, on the winglet, allowed it to perform well as a tip airfoil. The high lift produced gave the airfoil the ability to cruise at low angles of attack, further increasing the lift to drag ratio on the lift to drag ratio vs. velocity chart.
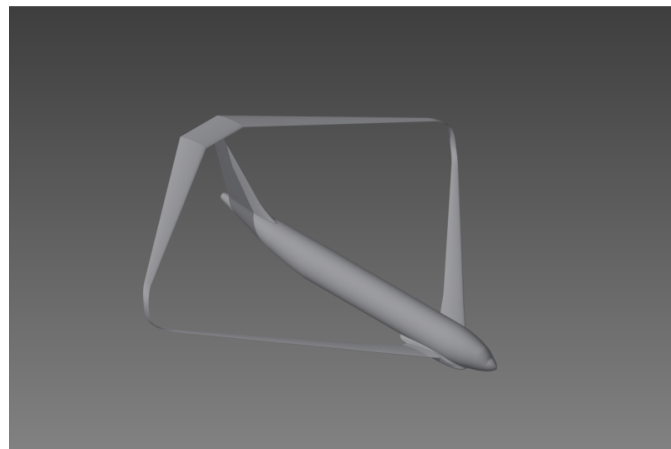
Figure 15. Maximum Winglet Height CAD Model
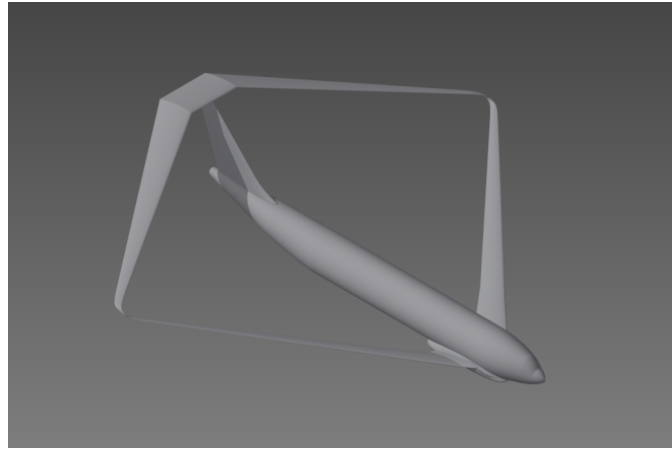
Figure 16. Minimum Winglet Height CAD Model

While overall the KC-135 Winglet performed the best, there are other trends to be noticed in the graphs. All of the box wing aircraft had a much smaller range of lift to drag ratios across different velocities in Fig. 16 when compared to the cantilever, suggesting that the box wing aircraft will perform better at off design point conditions. Comparing the box wing BAC J against the cantilever wing, this is especially noticeable in Fig. 11 (above), where the box wing BAC J has almost no change at all across change in angle of attack. The other box wing aircraft have little change in the lift to drag ratio vs. angle of attack as well, with the exception of the box wing KC-135 Winglet, the box wing designed, and the box wing Clark Y. The variations found in the Clark Y are likely due its nature of not being optimized for flow at such high Reynolds numbers. The reason for the other two box wings likely lies in the nature of the thin tip airfoils, which may reach flow separation more quickly than the airfoils with higher thickness to chord ratios. To mitigate the flow separation, a slightly lower angle of incidence could be utilized at the tip, at the expense of decreased lift production.

Winglet Height Optimization

An analysis of several different winglet heights is performed in the 2nd stage of optimization.

Winglet Height Optimization Methodology

The winglet height is initially defined as 20% of the span. A total of 7 different winglet height variations will be compared: 5% of span, 10%, 15%, 20%

(the baseline, original winglet height model), 25%, 30%, and 35%. The models require the same materials and are constructed similarly to the airfoil variation. All the models use the KC-135 Winglet airfoil that was determined to be the most efficient from testing in the preliminary airfoil optimization stage.

Winglet Height Optimization Results

Table 4

Lift results for Winglet Height Optimization

Lift (N)	0° Cruise	3° Cruise	225 m/s	237.5 m/s	250 m/s	262.5 m/s	275 m/s
35%	944633	1300392	1038575	1062000	1038266	1028138	1041706
30%	1001865	1274421	1036038	1050438	1032616	975464	933240
25%	924283	1283239	1042215	998399	1053269	1052677	1048857
20%	961772	1208696	1104278	1007362	1070683	1020063	939018
15%	939489	1310789	1043821	1054195	1052031	1021351	1058340
10%	973173	1259536	1035063	1024581	1069681	1014064	943367
5%	950181	1290368	1042375	1041880	1040425	1018671	1011664
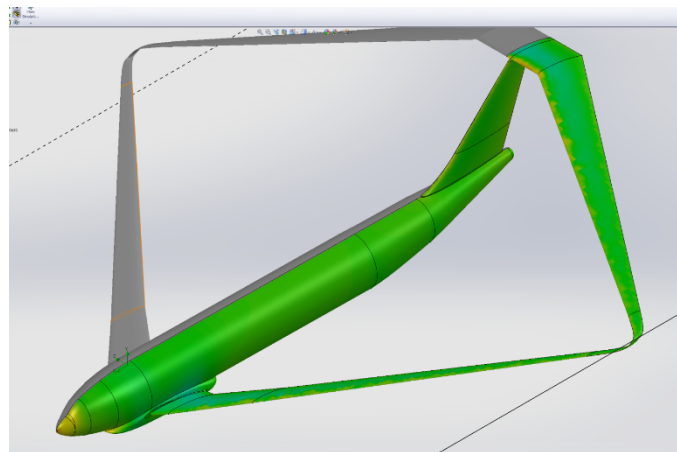
Figure 17. Minimum Winglet Height Pressure Plot. *1000-40,000 Pa*
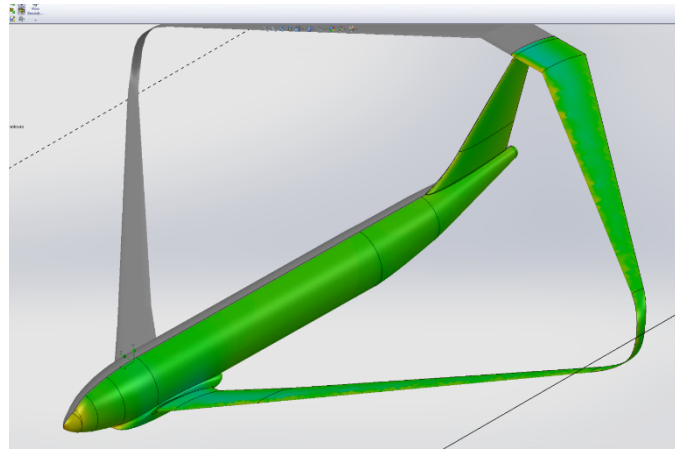
Figure 18. Maximum Winglet Height Pressure Plot. *1000-40,000 Pa*

Table 5

Drag results for Winglet Height Optimization

Drag (N)	0° Cruise	3° Cruise	225 m/s	237.5 m/s	250 m/s	262.5 m/s	275 m/s
35%	170937	247129	186159	185575	185234	194909	195120
30%	165650	249332	193981	181942	170502	167218	174628
25%	175693	244586	189506	183408	192762	193324	193048
20%	163942	244824	210304	194099	184513	187160	189559
15%	169458	246508	184559	184838	184236	191664	192730
10%	163755	249615	195997	193515	179560	180667	188568
5%	170790	242531	185859	183882	183527	190252	189330
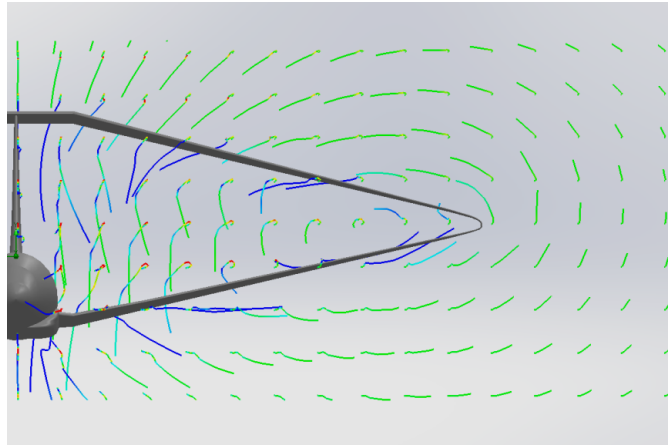
Figure 19. Minimum Winglet Height Flow Trajectory. *240-260 m/s*
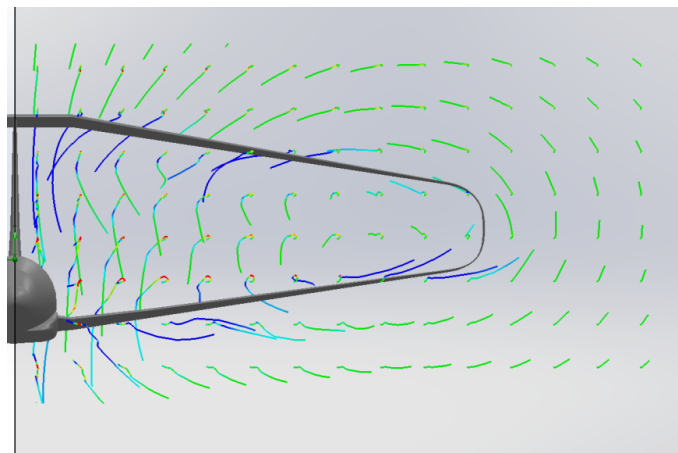
Figure 20. Maximum Winglet Height Flow Trajectory. *240-260 m/s*

Winglet Height Data Analysis

The variation of the winglet height resulted in a tighter data spread when compared to the airfoil variation, as expected; however, the difference between data points is significant enough. Overall, the model with 30% winglet height has the greatest lift to drag ratio. At cruise conditions it has a lift to drag ratio nearly 5% higher than the baseline model and 15% greater than the lift to drag ratio of the cantilever model. In every case tested, the 30% model outperforms the baseline model, and has the maximum lift to drag ratio in 4 out of the 7 total cases. The cases that the 30% model does not have the highest lift to drag ratio are

at 225, 275 m/s, and at 250 m/s 3 degrees angle of attack. Note that the results presented here are normalized with respect to the cantilever cruise condition, just as in the airfoil data analysis section.

The lift vs. angle of attack graph is quite linear, as displayed in Fig. 23. Overall, there is not a very significant trend in lift when comparing winglet height and lift. While the wing area is greater for the models with a smaller winglet height, the interference between the 2 wings not only affects the drag but also reduces the efficiency of the lift generation. As a result, the extra lift is partially cancelled out. The models that generated high lift simply had a beneficial balance of wing area and decreased interference.

In comparison to lift, drag vs. α is much less variable, shown in Fig. 24. Despite this, the combination of slight variations in drag and lift gave the overall lift to drag ratio vs. α a significant amount of variation in Fig. 25. Both the 35% and the 5% winglet heights had similar lift to drag ratios throughout the different angles of attack. Similarly, the 10% and the 30% behaved in this way. 15% and 25% had greater variation to start with in lift to drag ratio; however, at 3 degrees angle of attack the models converged on a similar lift to drag ratio. This suggests that there is a relation between lift to drag ratio and winglet height such that 20+X% and 20–X% have similar lift to drag ratios.

Analysis of the lift vs. velocity curve in Fig. 26 yields little variation, as the lift was normalized; however, it is noticeable that at the highest speed, 275 m/s, the 20%, 10%, and 30% all converge to a similarly low lift value, below what was expected. When the angle of attack is calculated for a certain speed, it is assumed that the relation between the lift coefficient and α is linear. The calculation of α for 275 m/s on these 3 models, 20%, 10%, and 30% all resulted in low angles of attack around -1.5 degrees, unlike the other 4 models, which all had angles of attack greater than -1 degrees. The negative angle of attack likely results in a large amount of interference between the fuselage and the wings, decreasing lift beyond its theoretical value.
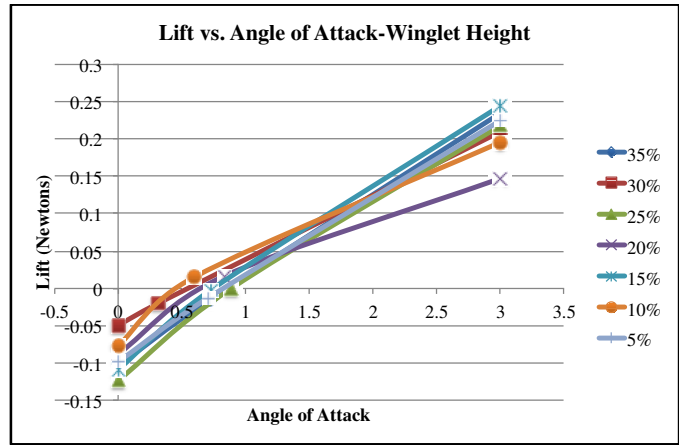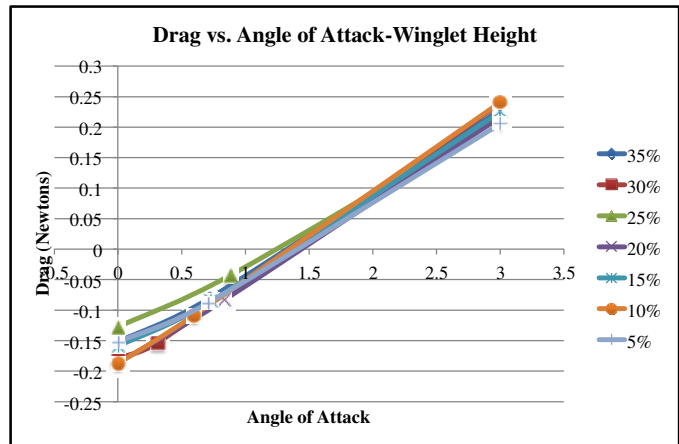
Figure 21. Lift vs. *α. Winglet Height*
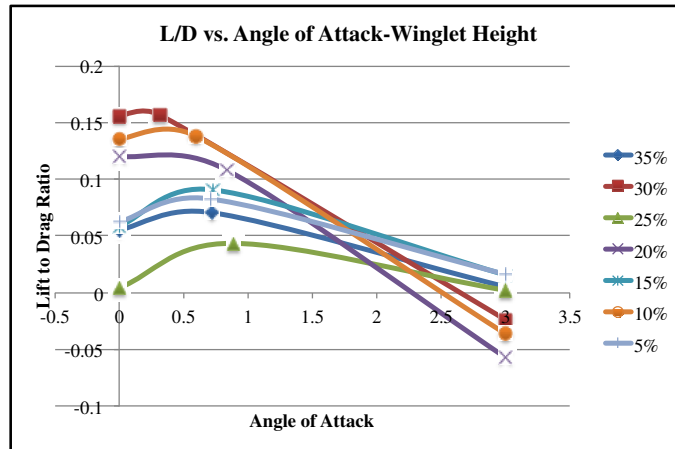

Figure 22. Drag vs. *α. Winglet Height*

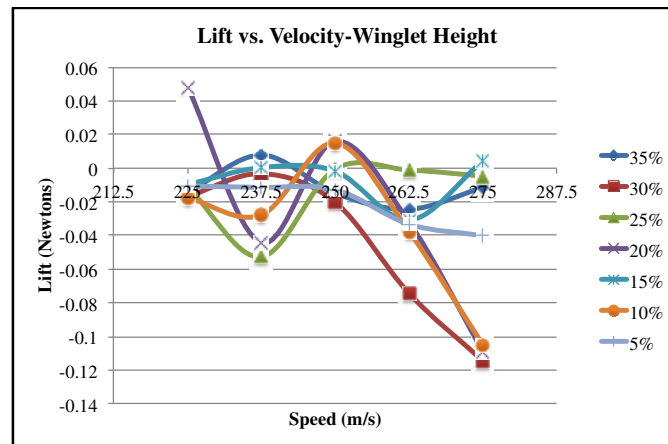*Figure 23*. Lift to Drag vs. *α. Winglet Height*

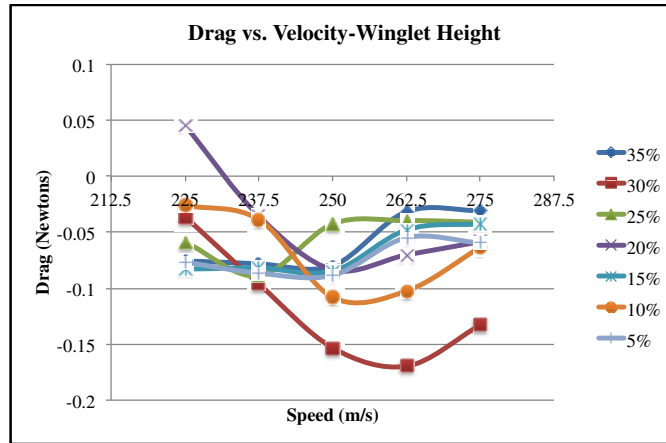*Figure 24*. Lift vs. Velocity. *Winglet Height*

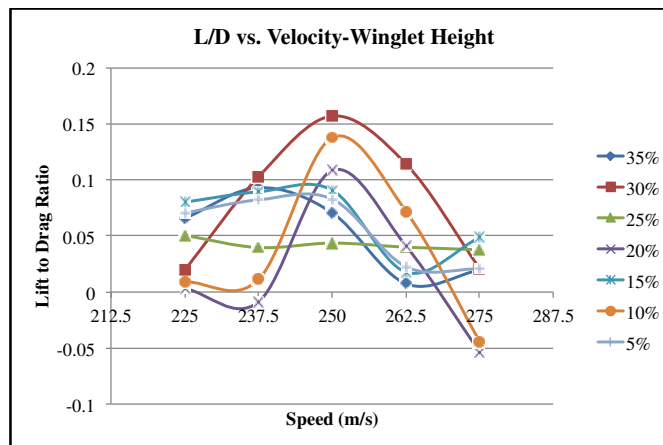*Figure 25*. Drag vs. Velocity. *Winglet Height.*

Figure 26. Lift to Drag vs. Velocity. *Winglet Height*

The drag values have significant variation when compared in Fig. 27 (below). The model with the least drag is the 30% model, likely helped as a result of decreased interference drag. Oddly, both the 5% and the 35% winglet height models have similar drag values. The other 4 all had drag values close to the control. It would be expected that the 35% winglet height model would have significantly less drag than 5%, especially considering the fact that the angle of attack values calculated were very similar. A reason for this would likely lie in the fact that the larger winglet itself generated more drag, which reduced the benefits of the decreased interference drag. Another important reason lies in the reduced wing area, which led to decreased lift production. The models which generate less

lift at 0 degrees and 3 degrees angle of attack, 250 m/s, such as this one, require a larger angle of attack to maintain the appropriate amount of lift at speed. The increased angle of attack would significantly increase parasitic drag from the fuselage. A combination of these two reasons increases the drag and decreases the lift to drag ratio of models such as the 35%.

The 15% and 25% winglet height have drag values that were fairly close in the Fig. 27, and the 10% model is closer to the 30% winglet height than any other model in terms of the shape of the trend. This suggests that 20+X% and 20–X% will be fairly similar in terms of drag. Examining Fig. 28, the lift to drag vs. velocity yields the same trend, excepting the 15% and 25% winglet height cases, due to the normalization of the lift. This supports the relation between lift to drag ratio and winglet height observed earlier. The reason why the relation is centered on 20% of the span may lie in the fact that it is close to the middle between the minimum winglet height, ~0%, and the maximum, which would likely be ~40% of the span such that the bottom wing does not have an anhedral angle.

Aspect Ratio Optimization

An analysis of several different aspect ratios is performed in the 3rd and final stage of optimization.

Aspect Ratio Optimization Methodology

A total of 7 different aspect ratio variations are compared. The baseline is the model tested with 30% winglet height and the KC-135 Winglet airfoil, determined to be the most efficient from the two previous iterations of design. The variations are done as a percentage increase or decrease in aspect ratio from the original. The 5 variations are: -15%, -10%, -5%, 0% (baseline), 5%, 10%, and 15%.

It is necessary to maintain a constant wing area in order to compare the different models, as all the models are being tested under conditions to produce the same amount of lift. In order to keep it constant, the original chord is divided by $\sqrt{1 + X\%}$ and the span is multiplied by the same ratio. An example calculation is presented below. Let b_x represent the span of the x% model and S_x be wing area. c_x is chord. For the 10% model:

$$S_{10} = b_{10} * c_{10} = \frac{b_0 * \sqrt{1.10}}{1} * \frac{c_0}{\sqrt{1.10}} = b_0 c_0 = S_0$$

$$AR_{10} = \frac{b_{10}^2}{S_{10}} = \frac{(b_0 * \sqrt{1.10})^2}{S_0} = \frac{b_0^2 * 1.10}{S_0} = AR_0 * 1.10$$

Thus the aspect ratio increased by 10% over the baseline and wing area stays constant, as expected. A total of 7 models are created in such a fashion and tested as outlined in the airfoil optimization section.

**Aspect Ratio Optimization Results**

Table 6

Lift results for Aspect Ratio Optimization

Lift (N)	0° Cruise	3° Cruise	225 m/s	237.5 m/s	250 m/s	262.5 m/s	275 m/s
15%	985904	1277212	1046573	1059107	1055594	1015426	919620
10%	951119	1295172	1036865	1034658	1036303	1002957	1046336
5%	950692	1238399	1090748	1067460	1073121	1018850	960168
0%	1001865	1274421	1036038	1050438	1032616	975464	933240
-5%	992310	1306774	1013254	1028272	1036558	1009699	942449
-10%	977159	1207822	1074692	1087063	1074803	995175	891272
-15%	940307	1269481	1036441	1029686	1048118	1005933	1006368

Table 7

Drag results for Aspect Ratio Optimization

Drag (N)	0° Cruise	3° Cruise	225 m/s	237.5 m/s	250 m/s	262.5 m/s	275 m/s
15%	178234	246383	187831	191179	189323	197378	190447
10%	171194	250967	202781	186362	191658	193194	200696
5%	165650	249332	193981	181942	170502	167218	174628
0%	165222	250929	186961	174206	172076	171585	187072
-5%	164874	234926	217652	190354	180937	176183	169439
-10%	178234	246383	187831	191179	189323	197378	190447
-15%	171194	250967	202781	186362	191658	193194	200696
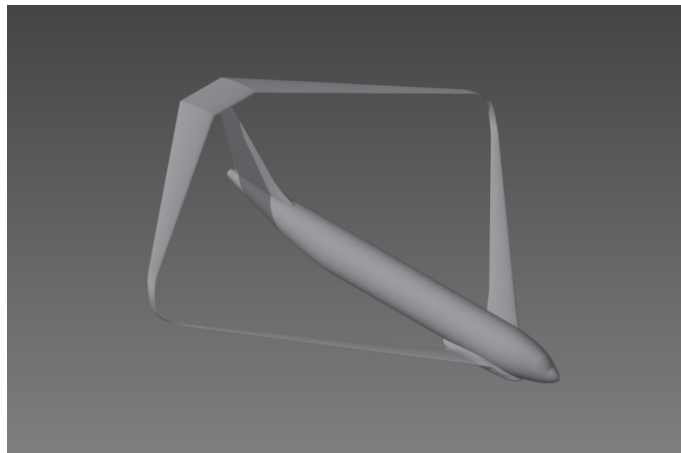
Figure 27. Minimum Aspect Ratio CAD Model.
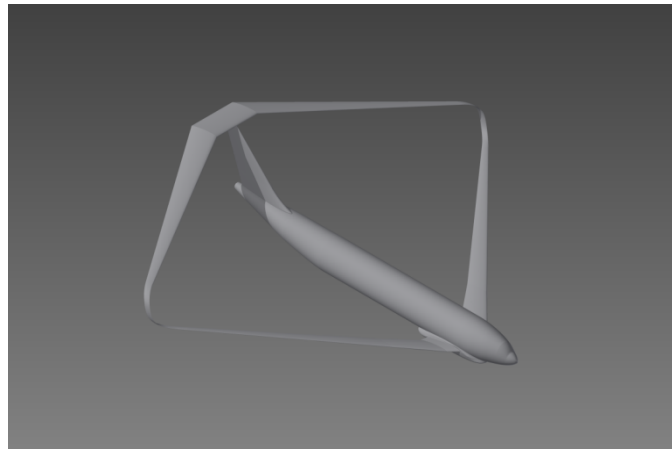
Figure 28. Maximum Aspect Ratio CAD Model
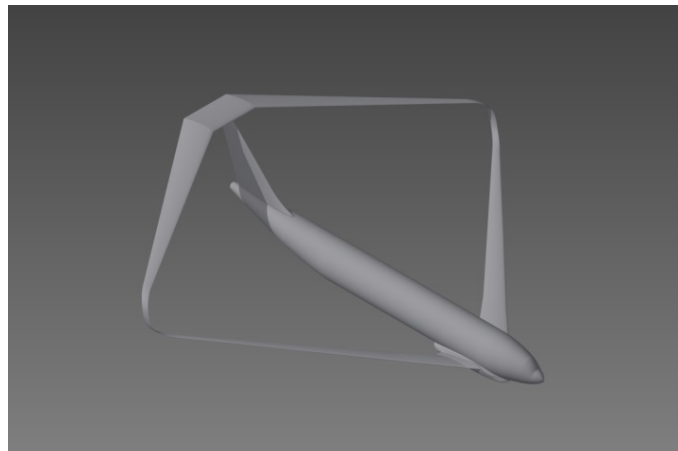
Figure 29. Optimized CAD Model
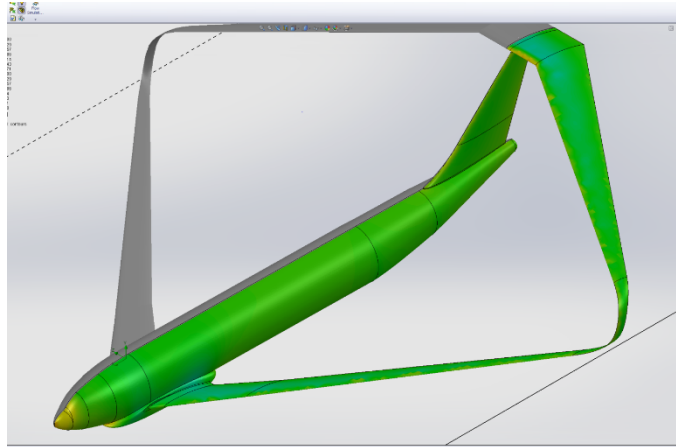
Figure 30. Minimum Aspect Ratio Pressure Plot. *1000-40,000 Pa*
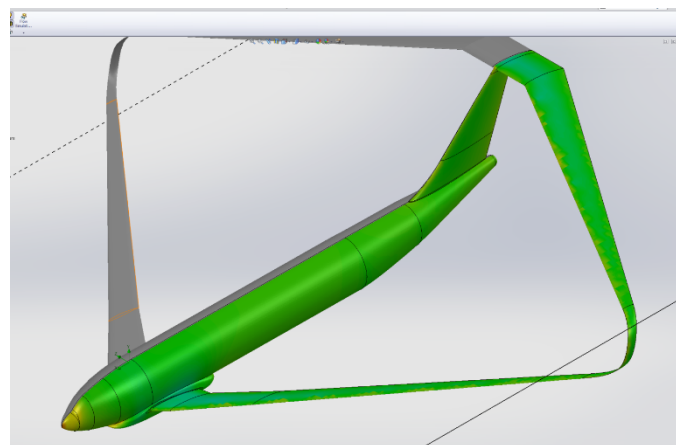
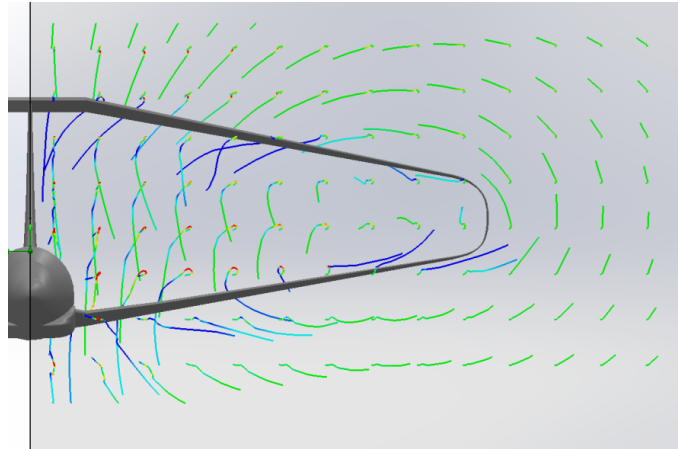*Figure 31.* Maximum Aspect Ratio Pressure Plot. *1000-40,000 Pa*

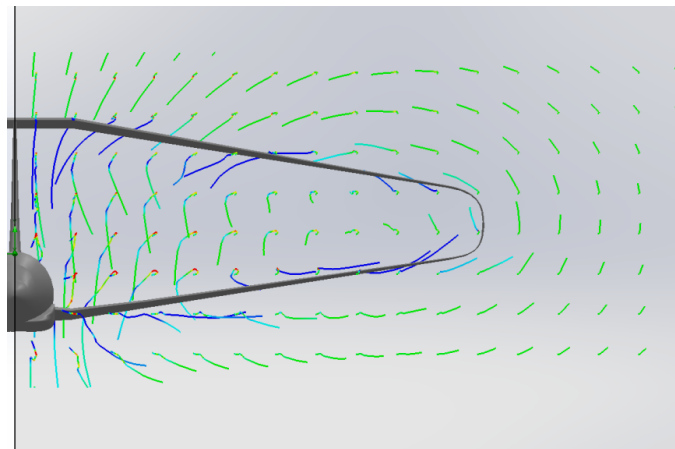*Figure 32.* Minimum Aspect Ratio Flow Trajectory. *240-260 m/s*

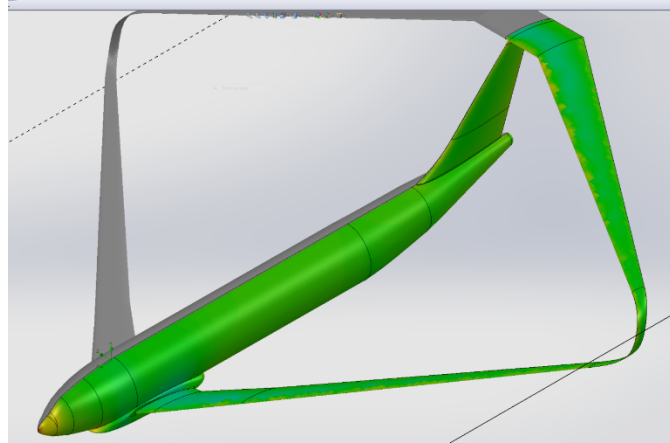*Figure 33.* Maximum Aspect Ratio Flow Trajectory. *240-260 m/s*

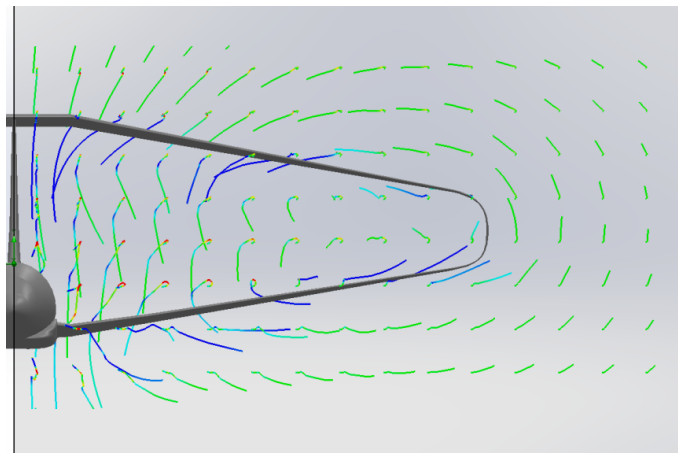*Figure 34*. Optimized Model Pressure Plot. *1000-40,000 Pa*

Figure 35. Optimized Model Flow Trajectory. *240-260 m/s*

Aspect Ratio Data Analysis

The results are once again normalized as before, and clearly show that both the -5% aspect ratio and the 0% baseline model perform the best. The two models have very similar lift to drag ratios at all the different cases, with the lift to drag values often being within 1% of one another. There were three main exceptions. At 250 m/s cruise conditions, 3 degrees angle of attack, and at 237.5 m/s, calculated angle of attack, the -5% aspect ratio model had a lift to drag ratio that was approximately 2% higher than the 0% aspect ratio model, visible in Fig. 38. In the case of 275 m/s, the 0% aspect ratio had a lift to drag ratio about 5% higher than the -5% aspect ratio. In addition, at 275 m/s the -15% and the 10%

aspect ratio model had the highest lift to drag ratio, about 2.5% higher than the 0% aspect ratio model. In all other cases, both the -5% and 0% had approximately the same lift to drag ratio and dominated the top of the charts in comparison to the rest of the models. Due to the very close results, a more precise analysis needs to be conducted to finalize results between the -5% and 0% aspect ratio models.
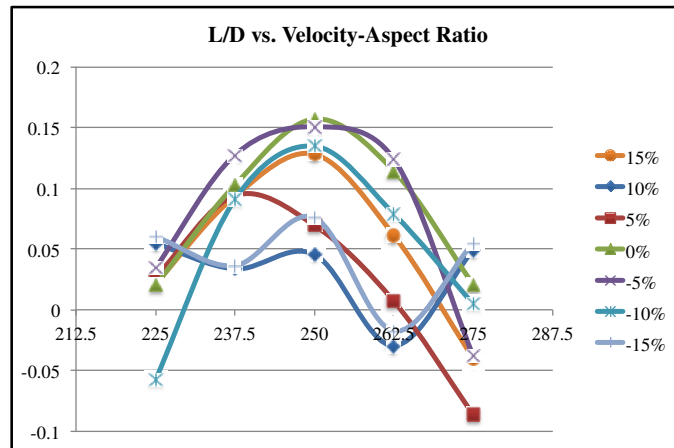

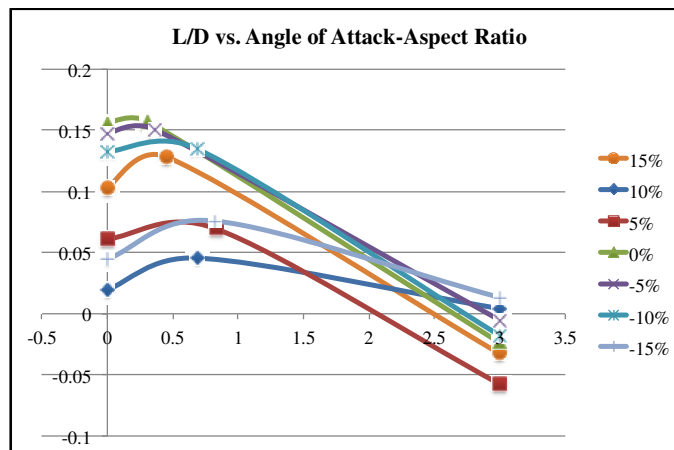
Figure 36. Lift to Drag vs. Velocity. *Aspect Ratio.*

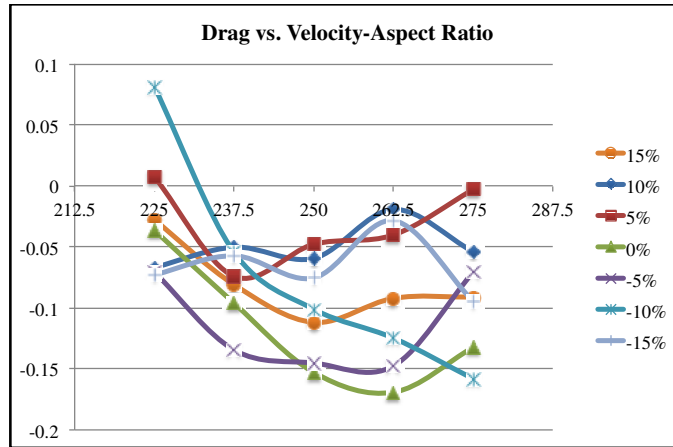*Figure 37*. Lift to Drag vs. *α. Aspect Ratio.*
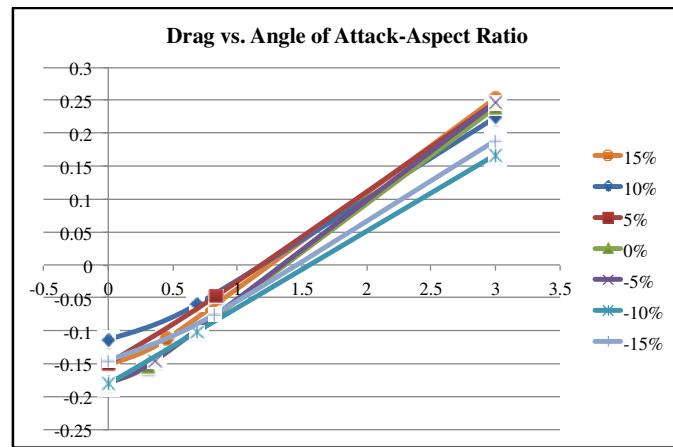
Figure 38. Drag vs. Velocity. *Aspect Ratio.*

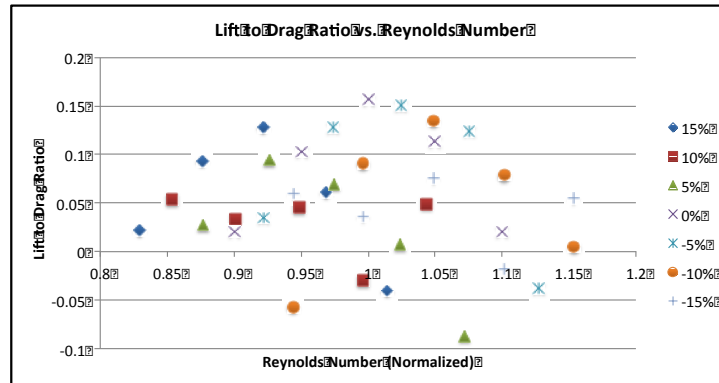*Figure 39*. Drag vs. *α. Aspect Ratio.*

Figure 40. Lift to Drag Ratio vs. Reynolds Number. The graph clearly shows that the lift to drag ratio peaks at a Reynolds number of approximately 1 (normalized).
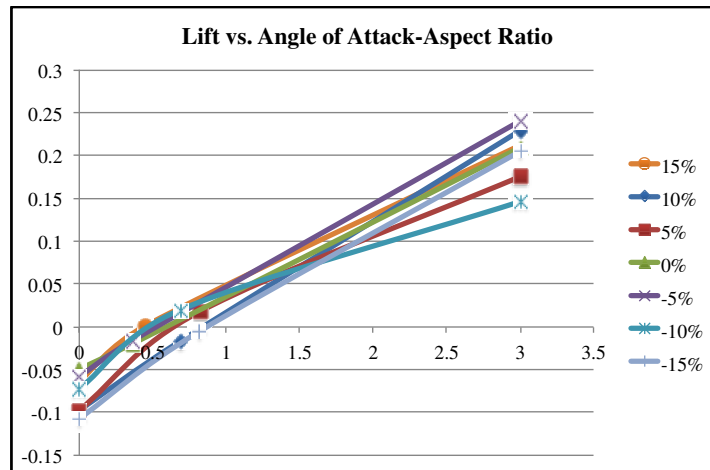

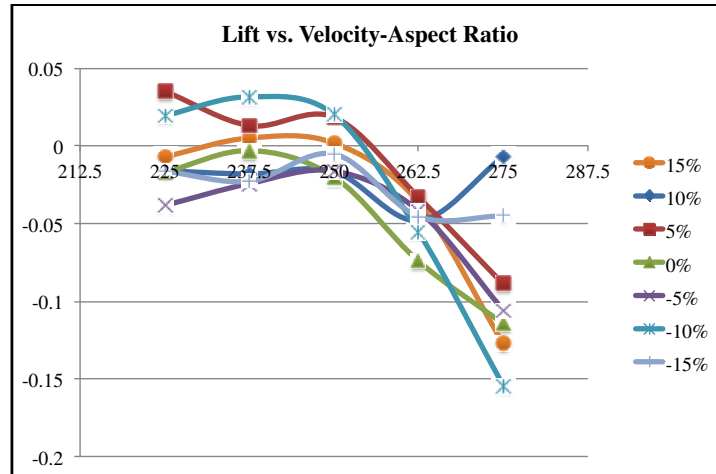*Figure 41*. Lift vs. *α. Aspect Ratio.*

Figure 42. Lift vs. Velocity. *Aspect Ratio.*

The poor performance of 5%, 10%, and 15% aspect ratio models is extremely surprising. These models should theoretically have low drag; the formula for induced drag shows how it is indirectly proportional to aspect ratio, and thus the expectation would be for the drag to decrease. As induced drag is expected to decrease, it must be parasitic drag that led to an increase in overall drag, for the overall drag is still quite high for the 5% and the 10% models. (See Fig. 38, 39)

The high parasitic drag of the 5% and 10% aspect ratio in Fig. 41 is more than likely influenced by two factors: frontal area and Reynolds number. The increase in span for the higher aspect ratios led to greater frontal area, which increases the drag. In addition, the decrease in chord (to keep a constant wing area) would have led to a change in Reynolds number, which likely was not optimal for this airfoil. Likely these two models had Reynolds numbers lower than what is needed. Similarly, the -10% model had Reynolds numbers higher than what is needed. The optimal position for Reynolds number and thus aspect ratio is likely between the cases of -5% aspect ratio and 0% aspect ratio, the baseline. Fig. 40 shows the relation between lift to drag ratio and Reynolds number for this data set. The values have been normalized with respect to 0% aspect ratio and 250 m/s cruise, or that the Reynolds number was set as 1 at that position.

While clearly the relation is not perfect, the highest lift to drag ratios seem to occur in the range from .95 to 1.05, which contains at 3 of the points from both

0% aspect ratio and 5% aspect ratio. This explains the good performance of these models. Examination of the Reynolds numbers also shows why the 10% aspect ratio model performed well at 275 m/s speed-it had a Reynolds number of 1.15, closer to the range than any other model at that speed.

The low lift production at 275 m/s cruise conditions (see Fig. 42) likely occurred in many models for similar reasons to the low lift production in winglet height: highly negative α values for those cruise conditions. The variation in the lift was much less here than in the comparison between winglet height and lift as a result of the wing area being kept constant.

The models may also produce less lift at high speeds as a result of the Reynolds number increase. The Reynolds number is assumed to be constant when producing the C_L vs. angle of attack relationship, and at higher numbers the models did not perform optimally.

Conclusion

The variation of the airfoil, then winglet height, and finally aspect ratio leads to a great increase in lift to drag ratio over the baseline design. The first step led to a lift to drag ratio increase of more than 20% over the baseline BAC-J box wing at 250 m/s cruise conditions, followed by a 5% increase through winglet height. The aspect ratio variation resulted in little improvement, with only the -5% aspect ratio model performing on par with the baseline. While the final step did not result in any improvements in lift to drag ratio, the experimentation did show that the optimal aspect ratio would be between -5% and 0% of aspect ratio of the baseline, giving a range for future experimentation (albeit with smaller gains). In addition, the optimized box wing (KC-135 Winglet, 30% winglet height, 0% aspect ratio) has over a 15% increase at cruise speed in lift to drag ratio over the cantilever wing model tested in the first phase of design, displaying the plausibility of box wing aircraft in the future. Additional testing and more design work on aspect ratio optimization and other parameters would likely lead to even higher lift to drag ratios.

Improvements that could be made to this experimentation include the design and testing of more airfoils in CFD, as well as scaled testing in a high-speed wind tunnel. In addition, while the CFD Validation study showed the accuracy of the lift calculation and the accuracy of the drag trend, other flow simulation software such as Fluent would provide more accurate drag calculations.

There is a large amount of further research that can be done. With the field of non-planar aircraft lacking much study, there is room to possibly analyze different airfoils in various other non-planar designs. In addition, optimization of the airfoil could be conducted on a lower speed, more fuel-efficient commercial aircraft design, or possibly a faster, supersonic transport. Lastly, the various other parameters, such as tip joined vs. inboard joined tips, can all be varied and optimized for the box wing aircraft, as this is simply a new field with much to study.

References

Abbot, I. H. (1959). *Theory of Wing Sections.* New York: Dover Publication.

Chiktanz, D. (Master's Thesis, Dept. of Automotive and Aeronautical Engineering, Hamburg University of Applied Sciences). *Conceptual Design of a Medium Range Box Wing Aircraft.* Hamburg, Germany: 2011.

Cornille, J. (1999). *Wind Tunnel Investigation of Joined Wing Configurations.* Dayton, OH.: Master's Thesis, Graduate School of Engineering, Air Force Institute of Technology Air University, Wright-Patterson AFB.

Cuerno-Rejado, C. A.-A. (2009). Conceptual Design of a Medium-sized Joined-wing Aircraft. *Proceedings of the Institution of Mechanical Engineers, Part G: Journal of Aerospace Engineering, Inst. Of Mechanical Engineers*, 681-696.

Gallman, J. W. (1993). Optimization of Joined-Wing Aircraft. *Journal of Aircraft, Vol. 30, No. 6*, 897-905. http://dx.doi.org/10.2514/3.46432

Kroo, I. (2005). *Nonplanar Wing Concepts for Increased Aircraft Efficienc.* California: VKI lecture series on Innovative Configurations and Advanced Concepts for Future Civil Aircraft, Stanford University.

Kroo, I. M. (2014, Jan 28). *Applied Aerodynamics: A Digital Textbook*. Retrieved from Desktop Aeronautics: http://www.desktop.aero/appliedaero/preface/welcome.html

Prandtl, L. (1924). *Induced Drag of Multiplanes.* NACA Technical Note No. 182.

Wolkovitch, J. (1986). The Joined Wing: An Overview. *Journal of Aircraft, Vol. 23, No. 3,*, 161-178. http://dx.doi.org/10.2514/3.45285

Appendix

Nomenclature

C_L	=	lift coefficient
$C_{L,MAX}$	=	maximum lift coefficient
C_D	=	drag coefficient
v	=	velocity
α	=	angle of attack
ρ	=	air density
υ	=	kinematic viscosity
Re	=	Reynolds number
c	=	wing chord length
S	=	wind planform area
T	=	temperature
P	=	pressure